Carbohydrate Polymers 86 (2011) 910–916

Contents lists available at ScienceDirect

Carbohydrate Polymers

journal homepage: www.elsevier.com/locate/carbpol

Biodegradable nanospheres self-assembled from complementary hydrophilic dextran macromers

Guoming Sun[a,1], Chih-Chang Chu[a,b,*]

[a] Fiber and Polymer Science Program, Department of Fiber Science & Apparel Design, Cornell University, Ithaca, NY 14853-4401, USA
[b] Department of Biomedical Engineering, Cornell University, Ithaca, NY 14853-5201, USA

ARTICLE INFO

Article history:
Received 31 March 2011
Received in revised form 9 May 2011
Accepted 24 May 2011
Available online 1 June 2011

Keywords:
Dextran
Self-assembly
Biodegradable
Nanosphere
Controlled release

ABSTRACT

Supramolecular self-assemblies are predominately driven by noncovalent molecular forces, and electrostatic interactions are the major force for charged molecules. In this paper, we demonstrate the self-assembly of hollow nanospheres from oppositely charged dextran-based hydrophilic macromers. Charged dextran derivatives were obtained by incorporating 2-bromoethylamine (Dex–BH) and chloroacetic acid (Dex–CA) into dextran. In a pH 5.0 buffer solution, Dex–BH and Dex–CA became protonated and deprotonated, respectively, and self-assembled into well-defined nanospheres. Dynamic light scattering (DLS) detected that these nanospheres have a uniform size distribution with a mean diameter of approximately 160 nm, but their size and distribution are largely dependent on molecular weight and pH value. Scanning electron microscopy (SEM) analysis revealed that these nanospheres could form a hollow architecture, which might be attributed to the hydrophilic characteristics of dextran macromers. An *in vitro* albumin release study indicates that the release rate reflects the nanosphere architecture, and further demonstrates their potential as drug delivery vehicles.

1. Introduction

Biodegradable polymeric nanospheres have received considerable interest because of their distinct advantages for drug delivery (Brannon-Peppas & Blanchette, 2004; Gref et al., 1994; Passarella et al., 2010). Nanospheres can penetrate deep into tissues through fine capillaries, cross the fenestration into interstitial space, and are easily taken up by cells via endocytosis/phagocytosis (Panyam & Labhasetwar, 2003). In addition, nanospheres can be delivered to distant and specific sites by localized delivery, which uses a catheter-based approach with a minimal invasive procedure (Song, Labhasetwar, Cui, Underwood, & Levy, 1998), or be directed to targeted tissues or organs by conjugating with targeting groups (Moghimi, Hunter, & Murray, 2001). Moreover, by coupling multifunctional groups onto nanospheres, for instance, nanospheres could simultaneously serve as drug delivery, cell imaging, and photothermal therapy (Guo et al., 2010).

Molecular self-assembly represents a significant advancement in the engineering of nanomaterials (Service, 2005; Zhang, 2002, 2003). Nanomaterials with diverse morphologies, such as vesicles, fibers, and tubules, have been fabricated through bottom-up molecular self-assembly (Antonietti & Förster, 2003; Park et al., 2006; Yan, Zhou, & Hou, 2004; Yokoi, Kinoshita, & Zhang, 2005). Zhang and Eisenberg (1995) even self-assembled a polystyrene-poly-(acrylic acid) block copolymer into six different morphological yet stable aggregates. In deed, most self-assembling polymeric spheres are formed from block copolymers. Gebhardt, Ahn, Venkatachalam, and Savin (2007) reported that poly(butadiene)-poly(L-lysine) could form spherical micelles in a high pH aqueous solution. As the pH decreases, the micelles swell due to charge–charge repulsions between corona chains and from the helix-coil transition of the poly(L-lysine) block. Diblock copolymers composed of azobenzene-containing polyacrylate and poly(acrylic acid) (PAzoM-b-PAA) have also been self-assembled into micro particles though H-aggregation by Zhao and co-workers (Su, Zhao, Wang, Li & Zhang, 2007). According to this study, the spherical particle could be transformed into a disk shape due to the disruption of H-aggregate when exposed to irradiation at 436 nm. Similarly, Liu and Jiang (2006) achieved a reversible self-assembled sphere using block copolymer poly(4-phenylazomaleinanil-co-4-vinylpyridine) and polybutadiene through hydrogen bonding interaction. They also found that visible light induced the cis-azobenzene units into trans-conformation, leading to intensive swelling of the core, thus generating hollow spheres. In addition to absolute self-assembly, a semi-self-assembly strategy was also used to form hollow spherical structures, such as through the removal of inner components of self-assembled micelles (Murthy, Ma, Clark, Remsen, & Wooley,

* Corresponding author at: Department of Biomedical Engineering, Cornell University, Ithaca, NY 14853-5201, USA. Tel.: +1 607 255 1938; fax: +1 607 255 1093.
E-mail address: cc62@cornell.edu (C.-C. Chu).
[1] Present address: Department of Chemical and Biomolecular Engineering, Johns Hopkins University, 3400 N Charles St., Baltimore, MD 21218, USA.

0144-8617/$ – see front matter © 2011 Elsevier Ltd. All rights reserved.
doi:10.1016/j.carbpol.2011.05.042

2001; Wang et al., 2002) and the direct synthesis of nanocapsules (Kim et al., 2010).

Recently, we demonstrated the self-assembly of tubular structures from hydrophilic dextran derivatives, i.e., dextran–bromoethylamine hydrobromide (Dex–BH) and dextran–carboxylic acid (Dex–CA) (Sun & Chu, 2009). These tubular self-assemblies were further impregnated into the hydrogel network to improve release properties (Sun & Chu, 2010). Interestingly, Dex–BH and Dex–CA were unable to self-assemble into distinct tubular structures at lower feeding concentrations (5.0 mg/mL). Based on our recent reports (Sun & Chu, 2009, 2010), we found that a shortage of Dex–BH and Dex–CA prevents the formation of tubular structures. Instead, to reach an energetically favorable state, we speculate that Dex–BH and Dex–CA can self-assemble into spherical architectures at a lower concentration.

Unlike hollow nanospheres self-assembled from amphiphilic polymers (Gebhardt et al., 2007; Matsui & Gologan, 2000; Zhang & Eisenberg, 1995), or those that require additional chemical reactions (Dou, Jiang, Peng, Chen, & Hong, 2003; Huang, Remsen, Kowalewski, & Wooley, 1999), both Dex–BH and Dex–CA are hydrophilic, so they follow a different self-assembling mechanism. As illustrated in Fig. 1, at lower concentrations, amine and carboxylic acid groups will become protonated and deprotonated, respectively, in an aqueous solution. Dex–BH and Dex–CA are thus oppositely charged and attract each other through electrostatic interactions. As both Dex–BH and Dex–CA are polyvalent, each of them has excess unpaired charged groups, they will further attract the other until they are depleted and thus form spherical architectures.

To explore the structure and potential applications of these aggregates, we synthesized a series of Dex–BH and Dex–CA with varying molecular weights. The influence of dextran molecular weight and the pH value of the solutions on the nanosphere size and distribution were investigated. The spherical structures were characterized by dynamic light scattering (DLS) and scanning electron microscopy (SEM). The correlation between the nanosphere formulation condition and the drug release was also examined.

2. Experimental methods

2.1. Materials

Dextran (MW = 6000, 40,000, 60,000) was purchased from Sigma Chemical Company (St. Louis, MO) and dried in a vacuum oven for 24 h at 50 °C before use. Dimethyl sulfoxide (DMSO), triethylamine, 2-bromoethylamine hydrobromide (BEAHB) and chloroacetic acid (CA) were purchased from Aldrich Chemical Company (Milwaukee, WI). BEAHB and CA were dried in a vacuum oven for 24 h at room temperature to remove moisture before use. Isopropanol was purchased from J.T. Baker (Philipsburg, NJ). Buffer solutions (pH 4.0, 5.0, and 7.0) were purchased from GFS chemicals (Powell, OH).

2.2. Synthesis of dextran macromers

The synthesis of dextran-2-bromoethylamine hydrobromide (Dex–BH) and dextran–chloroacetic acid (Dex–AC) were synthesized similarly according to our previous method (Sun & Chu, 2009), and the degree of substitution (DS, the number of substituting group per anhydroglucose unit) was also estimated according to previous study (Sun & Chu, 2006). To incorporate amine and carboxylic acid groups, dextran reacted with BEAHB and CA in the presence of triethylamine. An example of Dex–BH synthesis is given here. Briefly, pre-dried dextran (2.0 g) was first dissolved in anhydrous DMSO (20 mL) under nitrogen gas followed by injection of triethylamine (11.2 mL). Meanwhile, BEAHB (7.5 g) was dissolved in DMSO (10 mL) and subsequently added to the above solution. This solution was stirred for 5 h at 50 °C and then filtered. Dex–BH was then obtained by precipitating the filtered solution into excess cold isopropyl alcohol and further purified three times by dissolution and precipitation with DMSO and cold isopropyl alcohol, respectively. Before further use, Dex–BH was dried under vacuum overnight at room temperature. The DS of Dex–BH and Dex–CA obtained are approximately 2.15.

2.3. Self-assembly preparation

The self-assembly was achieved through the ionic interaction by mixing negatively charged Dex–CA and positively charged Dex–BH precursors. Equivalent concentrations (e.g., 0.5 mg/mL) of Dex–BH and Dex–CA solutions were first prepared using a buffer solution (pH 5.0) and mixed together, the mixed solution was then sonicated for 5 min (Branson 3510R-DTH sonicator, Branson, Danbury, CT, USA) after mixing. The mixed solution was stored for16 h at room temperature before being subjected to further tests. A series of self-assemblies were made and the solutions remained clear at lower concentrations, but became cloudy at higher concentrations. The self-assembling composition is expressed as DNSm-*p*-*c*. DNS stands for dextran nanosphere, m stands for the molecular weight of dextran (kDa), *p* stands for the pH value the solution, and *c* stands for the concentration of the precursors (mg/mL). For example, DNS40-5-0.05 is the nanosphere prepared from MW40000 dextran, at pH 5 with a concentration of 0.05 mg/mL.

2.4. Morphology

The morphology of the spheres was studied using scanning electron microscopy (SEM, Leica Cambridge Stereoscan 440, Cambridge, UK) in two modes: air dried and freeze dried. This self-assembling solution was dropped on the surface of the aluminum SEM stub and air dried. The SEM stub with the dried samples was then gold sputter-coated (JFC-1200 Fine Coater, Japan) for 15 s. The SEM examination was conducted at 25 kV accelerating voltage and 12 nA probe current. To reveal their morphology at an aqueous state, the solution was centrifuged, quickly frozen in liquid nitrogen, and then freeze-dried in a Virtis Freeze Drier (Gardiner, NY) for 3 days at −50 °C under vacuum. The specimen was spread onto an aluminum SEM stub with double-sided carbon tape, and the specimen was gold coated and observed the same way as described above.

2.5. Dynamic light scattering (DLS)

To determine the assembling sphere size, dynamic light scattering was performed with DynaPro LSR (Proterion Corporation, Piscataway, NJ, USA). Briefly, 100 μL of the sample solution was transferred into the testing cuvette and placed in the light scattering instrument. The experiment was measured at 25 °C with laser light wavelength of 826.2 nm at the angle of 90°, and the data were collected with the Dynamics program.

2.6. Drug release

Ovalbumin (OVA) was chosen as the model drug, and 5% OVA (w/w, OVA/polymers) was pre-loaded into the self-assembled spheres. First, 5% OVA was dissolved in a buffer solution (pH 5.0). Similar to the self-assembly process, equal concentrations of Dex–BH and Dex–CA (pH 5.0 buffer solution) were added successively to the OVA solution. Then, they were mixed and sonicated for 5 min in the sonicating water bath. The solution was stored for16 h at room temperature and centrifuged before release test.

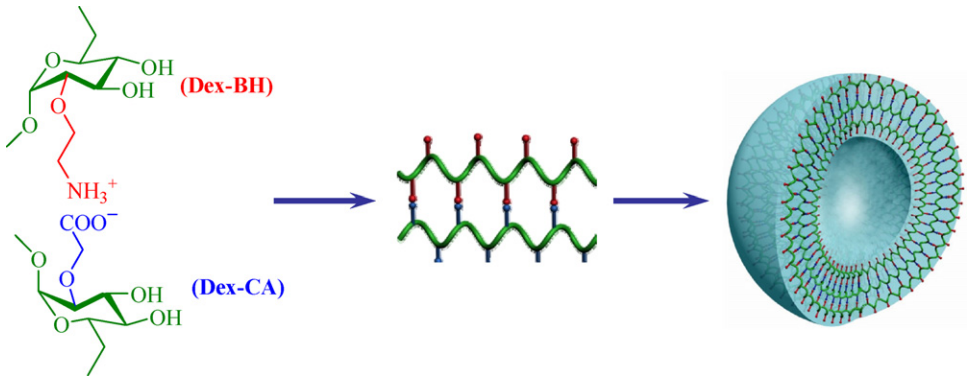

Fig. 1. Schematic illustration of sphere structures self-assembled from hydrophilic dextran macromers. Dex–BH and Dex–CA can become oppositely charged due to protonation and deprotonation in aqueous solution, respectively; they attract each other through electrostatic interactions to form spherical structures.

The QuantiPro Bicinchoninic Acid (QP-BCA) protein assay kit was used to determine the cumulative OVA release. The BCA assay solution was prepared according to the manufacturer's instructions. The OVA-loaded sphere was immersed in 1.0 ml PBS (pH 7.4) at 37 °C. At predetermined intervals, the solution was centrifuged; the supernatant was transferred to a capped glass vial; and 1.0 ml of bland PBS solution was added to the OVA-loaded specimen and then stirred. Meanwhile, 1.0 ml of the QP-BCA assay solution was added to the capped glass vial, mixed with the supernatant, and then incubated at 60 °C for 1 h. The samples were then transferred to a quartz cuvette, and the OVA concentration in PBS medium at each interval was monitored by the absorption of the medium at $\lambda = 560$ nm on a Perkin-Elmer Lambda 2 UV/VIS spectrometer (Norwalk, CT). The concentration of OVA released at a particular interval was calculated from an OVA standard calibration curve. All release studies were carried out in triplicate. The results are presented in the terms of cumulative release as a function of time:

$$\text{cumulative release}\,(\%) = \left(\frac{\sum_{t=0}^{t=t} M_t}{M_0}\right) \times 100$$

where $\sum_{t=0}^{t=t} M_t$ is the cumulative amount of released OVA from the assembling specimen at time t, and M_0 is the initial amount of loaded OVA.

3. Results and discussion

3.1. Spherical self-assembly

Amine and carboxylic acid groups become protonated and deprotonated in an aqueous solution, respectively. Dex–BH and Dex–CA become oppositely charged and attract each other through electrostatic attraction, the dominant force for these two precursors to self-assemble into ordered structures (Sun & Chu, 2009). The self-assembling solution was air dried for 2 h, and morphology was revealed by scanning electron microscopy (SEM). The SEM images in Fig. 2 indicate that spherical entities were self-assembled from the solutions with concentrations ranging from 0.01 mg/mL (DNS6-5-0.01) to 0.5 mg/mL (DNS6-5-0.5). At a higher concentration (DNS6-5-0.5), well-defined spherical structures with a large range of sizes were formed (Fig. 2A). At lower concentrations, the spherical structure became smaller and relatively uniform. Fig. 2B indicates that these spheres tend to aggregate at a concentration of 0.25 mg/mL (DNS6-5-0.25). With a further decrease in precursor concentration (DNS6-5-0.05), individual nanospheres were formed (Fig. 2C), but they started to lose their spherical structures at 0.01 mg/mL (DNS6-5-0.01, Fig. 2D).

The spherical self-assembly depends largely on the concentration of precursors. At a higher precursor concentration (e.g., DNS6-5-0.5), the self-assembled aggregates have more opportunity to interact with each other. Because these particles carry polyvalent charges, both positive and negative, these polyvalent particles can easily aggregate together to form a larger 3D sphere, as shown in Fig. 2A. The interaction between individual spheres was clearly evidenced in the precursor concentration of 0.25 mg/mL (DNS6-5-0.25, Fig. 2B). The SEM image revealed that two or more individual spheres aggregated together, indicating the existence of electrostatic forces or surface tension among the nanospheres at an appropriate concentration. When the concentration decreased to 0.05 mg/mL (DNS6-5-0.05), well-defined 3D nanospheres of uniform size formed (Fig. 2C). However, the self-assemblies lost their spherical structures, and some formed flat architectures when the concentration dropped to 0.01 mg/mL (DNS6-5-0.01, Fig. 2D).

In this study, the micro-sized self-assembled spheres (e.g., DNS-6-5-0.5) are beyond the dynamic light scattering (DLS) measurement, while no complete spherical structures can form at 0.01 mg/mL; thus the DLS measurement was performed at the concentration of 0.05 mg/mL.

3.2. Effect of MW of dextran on sphere size and distribution

Theoretically, any factors that influence the molecular interaction can affect molecular self-assembly. The higher molecular weight (MW) polymers have greater intermolecular forces, so an increase in MW can alter resultant nanosphere size. The self-assembled spheres at different dextran MWs were characterized by DLS; the data are shown in Fig. 3A. The average sphere size first increased from 129.7 ± 35.8 nm (Fig. 3Ai) to 158.8 ± 28.9 nm (Fig. 3Aiii) when the dextran MW increased from 6000 (DNS6-5-0.05) to 40,000 (DNS40-5-0.05), and then decreased to 131.0 ± 44.6 nm (Fig. 3Aii) when the dextran MW continued to increase to 60,000 (DNS60-5-0.05). However, the size distribution is wider at MW 6000 and 60,000 than at MW 40,000. This result verifies that the MW does have an influence on the sphere self-assembly in this system.

The change in nanosphere distribution from MW 6000 (DNS6-5-0.05) to MW 40,000 (DNS40-5-0.05) suggests that the increase in MW causes an increase in intermolecular forces to yield a uniform sphere distribution. Higher MW Dex–BH and Dex–CA become more polyvalent and attract oppositely charged molecules, leading to larger and uniform nanospheres. However, when the MW continued to increase, the sphere size distribution broadened. It is known that dextran is a linear polymer at a MW less than 40,000, but becomes an increasingly more branched polymeric structure as the MW increases beyond 40,000. Due to more steric effect,

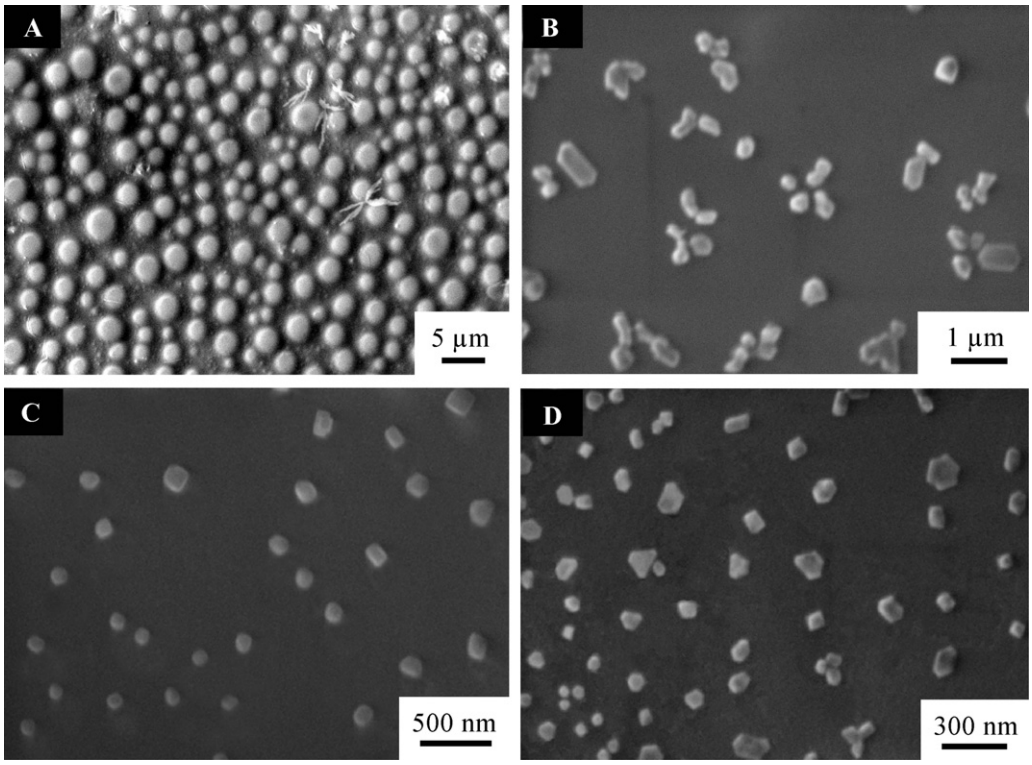

Fig. 2. SEM images of the self-assembled architectures from Dex–BH and Dex–CA at different concentrations. (A) DNS6-5-0.5, (B) DNS6-5-0.25, (C) DNS6-5-0.05, and (D) DNS6-5-0.01. Spherical structures were formed, but started to lose their morphology when Dex–BH and Dex–CA were depleted.

branched dextran does not have as strong interactions as the linear dextran does, which may contribute to the broader distribution. Moreover, the irregularity of the molecular structure may affect the distribution of ionic groups and therefore influence the sphere distribution as well. The increase in MW may also retard the molecular mobility and affect self-assembly. Molecular self-assembly seems very sensitive to the molecular weight change. Yan, Zhou, and Hou (2004) also found that molecular weight has an effect on the tubular self-assembly from HBPO-star-PEO molecules, and only those molecules with specific MW can self-assemble into tubular structures.

3.3. Effect of pH on sphere size and distribution

Electrostatic interactions are a major force for this spherical self-assembly. The nanosphere is dominated by the intermolecular forces between protonated amine groups and deprotonated carboxylic acid groups, of which their protonation/deprotonation depends on the pH value of their media. The effect of pH on sphere size and distribution is shown in Fig. 3A. The average particle size is about 104.7 ± 12.3 nm (DNS40-4-0.05) at pH 4.0 (Fig. 3iv) and 158.8 ± 28.9 nm (DNS40-5-0.05) at pH 5.0 (Fig. 3Aiii). Under these two conditions, the distribution is very narrow. However, when the pH increased to 7.0 (DNS40-7-0.05), though the average size is only 100.8 ± 58.1 nm (Fig. 3Av), the distribution is much broader than at pH4.0 (DNS40-4-0.05) or pH5.0 (DNS40-5-0.05).

The pH of the media has a distinct effect on the particle size and distribution. In aqueous media, both Dex–BH and Dex–CA are soluble, and the amine groups ($pK_a \sim 10.0$) and carboxylic acid groups ($pK_a \sim 3.0$) become protonated and deprotonated, respectively. Although the amine groups could become protonated in an aqueous solution, few of them would protonate in a neutral pH solution (i.e., pH 7.0), while most of the amine groups remain unprotonated. Thus, the interaction between the amine groups and carboxylic acid groups would not be strong enough to drive them to form uniform spherical structures at a higher pH. At a lower pH, the amine groups can become fully protonated, and the ionic interaction is much stronger, which more tightly binds the Dex–BH and Dex–CA, leading to smaller and more uniform nanospheres. Hu et al. (2002). also demonstrated a pH dependence on the formation of chitosan–poly(acrylic acid) nanoparticles, in which the particle size increased from 400 nm to 625 nm when the pH increased from 5.8 to 7.4, whereas the nanoparticles were completely destroyed at higher pH (pH > 9.0).

It is interesting to note that DNS40-5-0.05 in Fig. 3Aiii demonstrates a uniform size distribution. We were encouraged to investigate its morphology. Fig. 3B shows the well-defined spherical structures under this condition. Basically, there are two major sizes of nanospheres. The red arrows indicate the smaller spheres, which may correlate to the small peak observed at approximately 30 nm (Fig. 3Aiii). To further confirm their morphology, we analyzed the structure morphology at a higher magnification. Fig. 3C shows two distinct morphologies. The red arrows point to the smaller nanospheres, while most are uniform larger nanospheres, which is consistent with the morphology of Fig. 3B. As these nanospheres were self-assembled in an aqueous solution, a longer exposure time to air during the drying process may have resulted in some loss of actual morphology. This further encourages us to examine their interior morphologies under a freeze-dried condition.

3.4. Interior morphology of the nanospheres

To determine interior morphology, the centrifuged nanosphere solution was quickly frozen in liquid nitrogen, freeze-dried; and analyzed using SEM, as shown in Fig. 4. The process of quick freezing in liquid nitrogen allowed preservation of the interior morphology. The SEM images displayed in Fig. 4A (DNS40-5-0.5) through Fig. 4C (DNS40-5-0.05) show more details about these spheres. Similar to the structures reported by Xia and co-workers (Hyuk Im, Jeong,

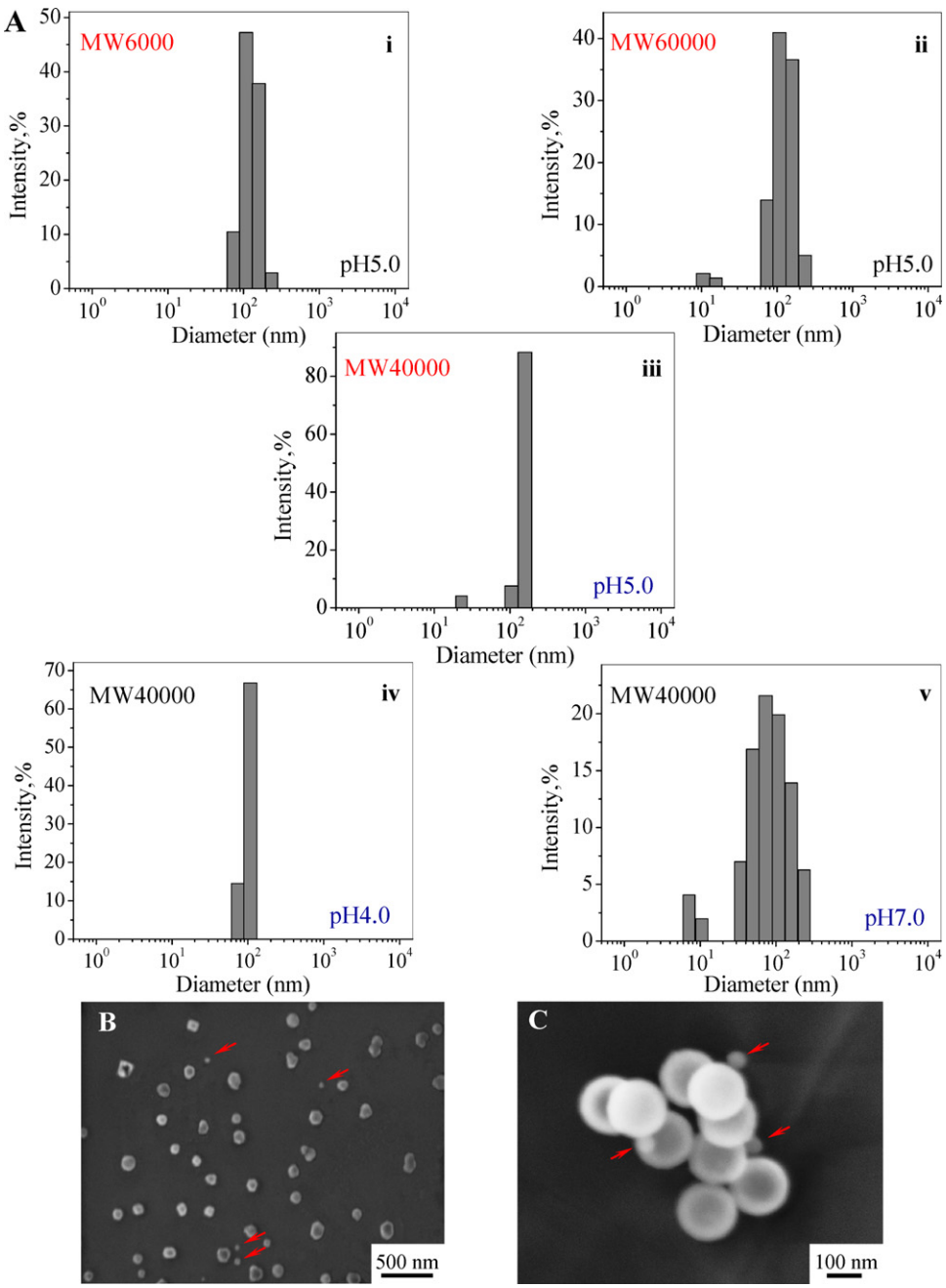

Fig. 3. Size determination of the biodegradable dextran nanospheres. (A) Effect of MW and pH on the particle size and distribution (i) DNS6-5-0.05, $d = 129.7 \pm 35.8$ nm, (ii) DNS60-5-0.05, $d = 131.0 \pm 44.6$ nm, (iii) DNS40-5-0.05, $d = 158.8 \pm 28.9$ nm, (iv) DNS40-4-0.05, $d = 104.7 \pm 12.3$ nm, and (v) DNS40-7-0.05, $d = 100.8 \pm 58.1$ nm. Only the diameters of the nanostructures are measured. The size of microstructures is beyond the instrument measurement and not shown in this graph. (B) SEM image of DNS40-5-0.05 after air-drying for 2 h. (C) SEM image of DNS40-5-0.05 at higher resolution after air-drying for 30 min.

& Xia, 2005), Figs. 4A (DNS40-5-0.5) and 4B (DNS40-5-0.25) illustrate two distinct morphologies: hemispheres and near-complete spheres. These morphologies were not revealed by the air-drying procedure, during which these structures may have been dehydrated, thus losing their original structure. When the concentration decreased, the nanospheres became much smaller and more uniform (Fig. 4C, DNS40-5-0.05). In addition to the hemisphere, there were also some cracked nanospheres. Fig. 4Di and Dii (DNS40-5-0.05) shows the typical structures of cracked nanospheres at a higher magnification. This result indicates that self-assembling is a dynamic process, and different stages coexist in each system. Moreover, this self-assembling can occur as hollow structures.

In addition to the hollow nature of the spherical particles, the SEM images also revealed that the shell thickness of the nanospheres varied under different concentrations. Unlike bilayer nanospheres or tubules formed through the hydrophobic interactions (Santoso, Hwang, Hartman, & Zhang, 2002; von Maltzahn, Vauthey, Santoso, & Zhang, 2003), which had uniform layer thickness, the nanospheres in this study had a wide range of shell thicknesses. This is attributed to the polyvalent characteristics of the dextran derivatives, from which they could attract each other and form thick layers. Therefore, this result further supports our hypothesis in Fig. 1.

The coexistence of hemisphere and complete nanospheres encourages us to further explore the interior structure. To examine our hypothesis that the self-assembling nanosphere is a dynamic process, we compared two self-assembling structures (DNS40-5-0.05) at 2 h and 16 h (Fig. 5). Fig. 5A indicates that plate (or

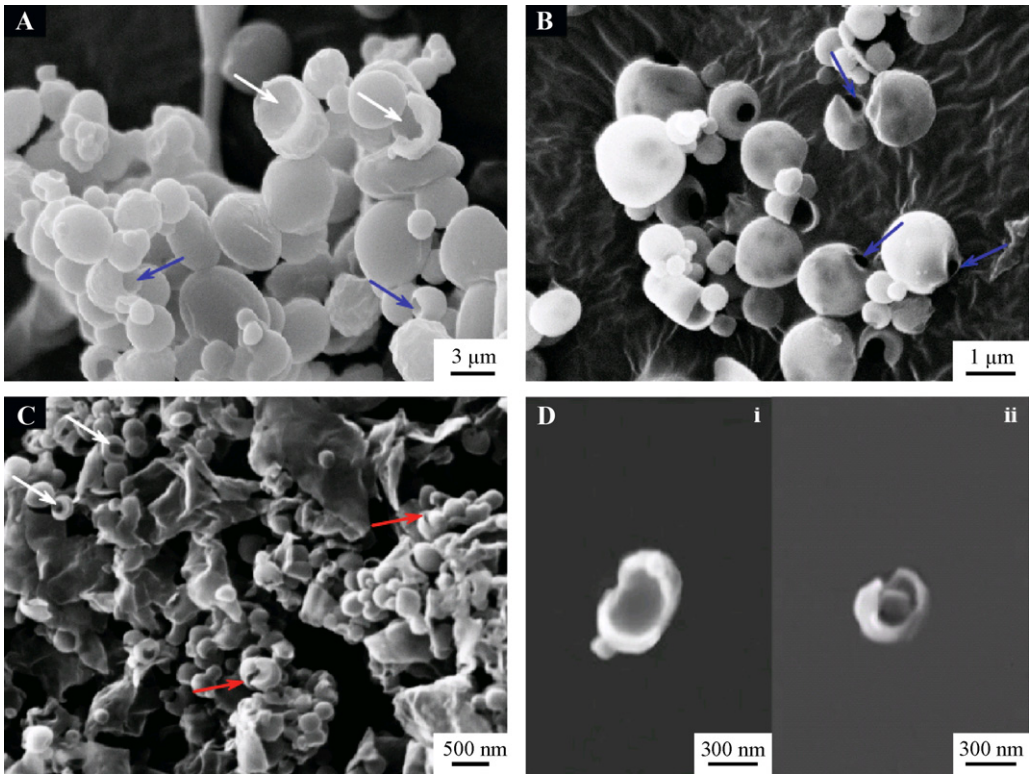

Fig. 4. The SEM micrograph of the freeze-dried spherical self-assembles at different concentrations. (A) DNS40-5-0.5, (B) DNS40-5-0.25, (C) DNS40-5-0.05, Di and Dii typical structures of broken DNS40-5-0.05. The interior structures were revealed, and hollow sphere were formed at various concentrations. (White arrows indicate the formation of hemisphere; blue arrows indicate near-complete spheres; red arrows indicate the cracked spheres). (For interpretation of the references to color in this figure legend, the reader is referred to the web version of the article.)

half-bowl)-like structures formed within 2 h, while Fig. 5B reveals that more complete spherical structures formed within 16 h.

We speculate that the hollow structure is attributed to the hydrophilic properties of the dextran derivatives. As both Dex–BH and Dex–CA are polyvalent, there are excess amine and carboxyl groups available when they are mixed and self-assembled, which makes the self-assembled aggregates hydrophilic and charged. As a result, when self-assembling nanospheres, both the inner and outer layers of the sphere are hydrophilic (i.e., both layers try to remain in the aqueous media). This is much like bilayer spheres, in which the hydrophobic tails pack tightly toward each other, while the hydrophilic heads pack against each other toward the surface. While both Dex–BH and Dex–CA are hydrophilic polymers, their surfaces are hydrophilic when they form layers. Consequently, the spheres become hollow. At a relatively higher precursor concentration, more molecules are attracted to the spherical aggregates and thus form larger spheres.

3.5. Cumulative release test

To evaluate the self-assembled spheres as drug carriers, 5.0% (w/w) OVA was pre-loaded into the spheres (DNS40-50.05). The cumulative release was observed for 60 days and results are shown in Fig. 6. The release profile in Fig. 6 presents two distinct stages: the first stage shows a relatively faster release, with approximately 60% OVA released in the 10 days; the second stage released about 40% OVA over 50 days.

Because of it hydrophilic characteristics, OVA tends to distribute on the hydrophilic layer of the self-assembled nanospheres. The faster release of the first stage could be attributed to the OVA

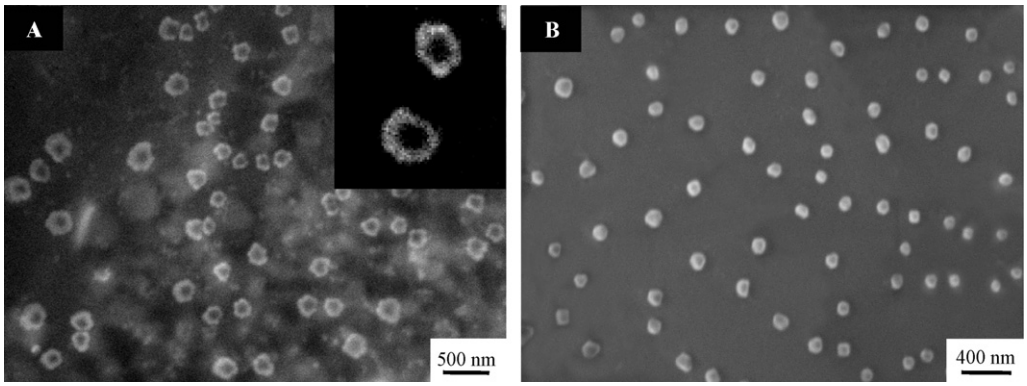

Fig. 5. SEM images of nanostructures (DNS40-5-0.05) self-assembled within (A) 2 h and (B) 16 h. Plate- or half-bow-like nanostructures self-assembled within 2 h, while complete nanosphere structures formed after 16 h.

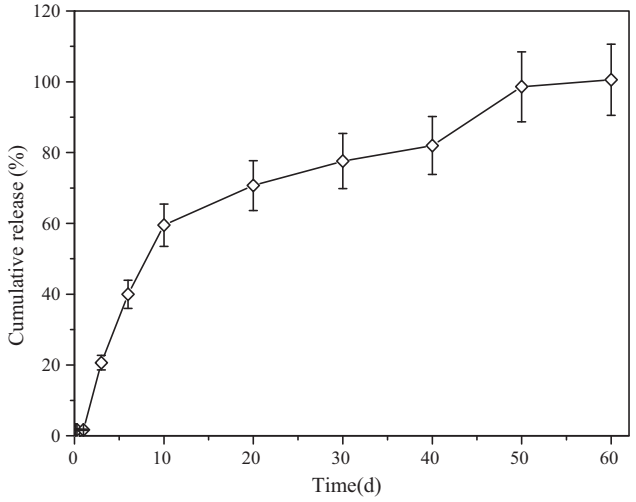

Fig. 6. Cumulative release of OVA from self-assembled nanospheres (DNS40-5-0.05).

distribution located in the outer layer of the nanospheres. As the nanospheres degrade, the OVA trapped between the layers released slowly. The remaining OVA released quickly when the nanospheres completely degraded.

4. Conclusions

Nanospheres can self-assemble from hydrophilic Dex–BH and Dex–CA in an aqueous solution. Their morphology, size, and distribution are largely dependent on the precursor concentration, the molecular weight of dextran, and the pH values of the solutions. The morphology study by SEM reveals that nanospheres can form hollow structures. We suggest that these hollow structures are attributed to the hydrophilicity of Dex–BH and Dex–CA: because Dex–BH and Dex–CA are hydrophilic, both the inner and the outer layers are hydrophilic, so the nanospheres formed in aqueous solution are thus hollow. The *in vitro* albumin release study indicated that the release rate reflects the nanosphere architecture, and further demonstrates their potential for controlled release in drug delivery application.

In addition, as amine and carboxyl groups are introduced into dextran, it is possible to incorporate other functional or targeting molecules by further chemical reaction or physical bonding. With the incorporation of targeting groups, this nanosphere may find a large range of applications.

Acknowledgement

We are grateful for the financial support of College of Human Ecology (assistantship to G. Sun) that made the study possible.

References

Antonietti, M., & Förster, S. (2003). Vesicles and liposomes: A self-assembly principle beyond lipids. *Advanced Materials*, *15*(16), 1323–1333.

Brannon-Peppas, L., & Blanchette, J. O. (2004). Nanoparticle and targeted systems for cancer therapy. *Advanced Drug Delivery Reviews*, *56*(11), 1649–1659.

Dou, H., Jiang, M., Peng, H., Chen, D., & Hong, Y. (2003). pH-dependent self-assembly: Micellization and micelle-hollow-sphere transition of cellulose-based copolymers. *Angewandte Chemie International Edition*, *42*(13), 1516–1519.

Gebhardt, K. E., Ahn, S., Venkatachalam, G., & Savin, D. A. (2007). Rod-sphere transition in polybutadiene–poly(L-lysine) block copolymer assemblies. *Langmuir*, *23*(5), 2851–2856.

Gref, R., Minamitake, Y., Peracchia, M., Trubetskoy, V., Torchilin, V., & Langer, R. (1994). Biodegradable long-circulating polymeric nanospheres. *Science*, *263*(5153), 1600–1603.

Guo, R., Zhang, L., Qian, H., Li, R., Jiang, X., & Liu, B. (2010). Multifunctional nanocarriers for cell imaging, drug delivery, and near-IR photothermal therapy. *Langmuir*, *26*(8), 5428–5434.

Hu, Y., Jiang, X., Ding, Y., Ge, H., Yuan, Y., & Yang, C. (2002). Synthesis and characterization of chitosan–poly(acrylic acid) nanoparticles. *Biomaterials*, *23*(15), 3193–3201.

Huang, H., Remsen, E. E., Kowalewski, T., & Wooley, K. L. (1999). Nanocages derived from shell cross-linked micelle templates. *Journal of the American Chemical Society*, *121*(15), 3805–3806.

Hyuk Im, S., Jeong, U., & Xia, Y. (2005). Polymer hollow particles with controllable holes in their surfaces. *Nature Materials*, *4*(9), 671–675.

Kim, D., Kim, E., Lee, J., Hong, S., Sung, W., Lim, N., et al. (2010). Direct synthesis of polymer nanocapsules: Self-assembly of polymer hollow spheres through irreversible covalent bond formation. *Journal of the American Chemical Society*, *132*(28), 9908–9919.

Liu, X., & Jiang, M. (2006). Optical switching of self-assembly: Micellization and micelle-hollow-sphere transition of hydrogen-bonded polymers. *Angewandte Chemie International Edition*, *45*(23), 3846–3850.

Matsui, H., & Gologan, B. (2000). Crystalline glycylglycine bolaamphiphile tubules and their pH-sensitive structural transformation. *The Journal of Physical Chemistry B*, *104*(15), 3383–3386.

Moghimi, S. M., Hunter, A. C., & Murray, J. C. (2001). Long-circulating and target-specific nanoparticles: Theory to practice. *Pharmacological Reviews*, *53*(2), 283–318.

Murthy, K. S., Ma, Q. G., Clark, C. G., Remsen, E. E., & Wooley, K. L. (2001). Fundamental design aspects of amphiphilic shell-crosslinked nanoparticles for controlled release applications. *Chemical Communications*, *8*, 773–774.

Panyam, J., & Labhasetwar, V. (2003). Biodegradable nanoparticles for drug and gene delivery to cells and tissue. *Advanced Drug Delivery Reviews*, *55*(3), 329–347.

Park, C., Lee, I. H., Lee, S., Song, Y., Rhue, M., & Kim, C. (2006). Cyclodextrin-covered organic nanotubes derived from self-assembly of dendrons and their supramolecular transformation. *Proceedings of the National Academy of Sciences of the United States of America*, *103*(5), 1199–1203.

Passarella, R. J., Spratt, D. E., van der Ende, A. E., Phillips, J. G., Wu, H., Sathiyakumar, V., et al. (2010). Targeted nanoparticles that deliver a sustained, specific release of paclitaxel to irradiated tumors. *Cancer Research*, *70*(11), 4550–4559.

Santoso, S., Hwang, W., Hartman, H., & Zhang, S. (2002). Self-assembly of surfactant-like peptides with variable glycine tails to form nanotubes and nanovesicles. *Nano Letters*, *2*(7), 687–691.

Service, R. F. (2005). How far can we push chemical self-assembly? *Science*, *309*(5731), 95–195.

Song, C., Labhasetwar, V., Cui, X., Underwood, T., & Levy, R. J. (1998). Arterial uptake of biodegradable nanoparticles for intravascular local drug delivery: Results with an acute dog model. *Journal of Controlled Release*, *54*(2), 201–211.

Su, W., Zhao, H., Wang, Z., Li, Y., & Zhang, Q. (2007). Sphere to disk transformation of micro-particle composed of azobenzene-containing amphiphilic diblock copolymers under irradiation at 436 nm. *European Polymer Journal*, *43*(2), 657–662.

Sun, G., & Chu, C.-C. (2006). Synthesis, characterization of biodegradable dextran-allyl isocyanate-ethylamine/polyethylene glycol–diacrylate hydrogels and their in vitro release of albumin. *Carbohydrate Polymers*, *65*(3), 273–287.

Sun, G., & Chu, C.-C. (2009). Self-assembly of chemically engineered hydrophilic dextran into microscopic tubules. *ACS Nano*, *3*(5), 1176–1182.

Sun, G., & Chu, C.-C. (2010). Impregnation of tubular self-assemblies into dextran hydrogels. *Langmuir*, *26*(4), 2831–2838.

von Maltzahn, G., Vauthey, S., Santoso, S., & Zhang, S. (2003). Positively charged surfactant-like peptides self-assemble into nanostructures. *Langmuir*, *19*(10), 4332–4337.

Wang, M., Jiang, M., Ning, F., Chen, D., Liu, S., & Duan, H. (2002). Block-copolymer-free strategy for preparing micelles and hollow spheres: Self-assembly of poly(4-vinylpyridine) and modified polystyrene. *Macromolecules*, *35*(15), 5980–5989.

Yan, D., Zhou, Y., & Hou, J. (2004). Supramolecular self-assembly of macroscopic tubes. *Science*, *303*(5654), 65–67.

Yokoi, H., Kinoshita, T., & Zhang, S. (2005). Dynamic reassembly of peptide RADA16 nanofiber scaffold. *Proceedings of the National Academy of Sciences of the United States of America*, *102*(24), 8414–8419.

Zhang, L., & Eisenberg, A. (1995). Multiple morphologies of "crew-cut" aggregates of polystyrene-b-poly(acrylic acid) block copolymers. *Science*, *268*(5218), 1728–1731.

Zhang, S. (2002). Emerging biological materials through molecular self-assembly. *Biotechnology Advances*, *20*(5–6), 321–339.

Zhang, S. (2003). Fabrication of novel biomaterials through molecular self-assembly. *Nature Biotechnology*, *21*(10), 1171–1178.